JOURNAL OF CHEMICAL EDUCATION

pubs.acs.org/jchemeduc

Demonstration

Intermolecular $\pi-\pi$ Stacking Interactions Made Visible

Brian Jacobus Jozefus Timmer and Tiddo Jonathan Mooibroek*

Cite This: *J. Chem. Educ.* 2021, 98, 540–545

Read Online

ACCESS | Metrics & More | Article Recommendations | Supporting Information

ABSTRACT: Mixing the liquids hexafluorobenzene (**1**) and 1,3,5-trimethylbenzene (mesitylene, **2**) results in a crystalline solid with a melting point of 34 °C. The solid consists of alternating $\pi-\pi$ stacked pillars of both aromatics. This simple experiment can be used to visually demonstrate the existence and the effect of noncovalent intermolecular $\pi-\pi$ stacking interactions. Both benzene derivatives are relatively benign and widely available, and the experiment can be performed within minutes for less than $15 when done on a 22 mL scale (total volume). The demonstration is very robust, as **1**:**2** mixtures in volume ratios between 2/3 and 3/2 all give a visually similar result (molar ratios of 1.8–0.8). Substituting **2** with the liquid aromatics *o*-xylene, *p*-xylene, and aniline also resulted in the formation of a crystalline solid, while using many other liquid aromatics did not.

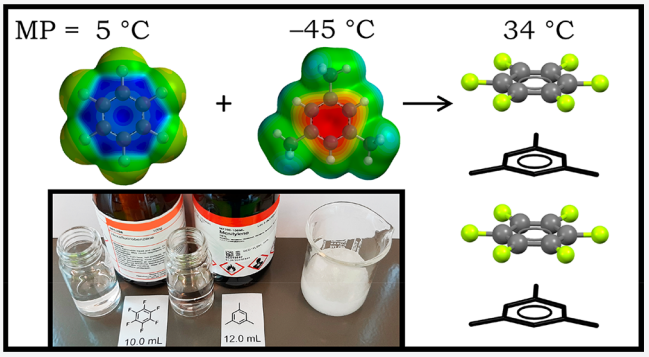

KEYWORDS: *Noncovalent Interactions, Crystals/Crystallography, Molecular Recognition, Molecular Biology, General Public, Demonstrations, Analogies/Transfers, Inquiry-Based/Discovery Learning*

Hydrogen bonds are well-known noncovalent interactions that largely drive supramolecular recognition phenomena such as base-pairing in double stranded DNA, protein binding, cell–cell recognition, and viral infection.[1−3] For example, infection of the pandemic causing SARS-CoV-2 begins when its spike proteins bind to a cell membrane enzyme (ACE2) via several hydrogen bonds.[4]

There are many other noncovalent interactions known in the scientific literature,[5−13] but these are largely unknown to high school students and undergraduates. An important class of molecules that engage in specific intermolecular interactions are aromatic rings.[14] Such conjugated π-systems typically have an electron rich center (i.e., π-basic) that can interact with H atoms such as the weakly polarized C–H hydrogen atoms of carbohydrates.[15,16] The center of an aromatic ring can also be rendered electron deficient (i.e., π-acidic), which allows it to interact with electron rich partners such as anions.[17−19] Interactions with aromatic rings are highly relevant to biology, where such interactions commonly occur with the nucleobases and the aromatic amino acid residues.[20,21] When π-systems stack with themselves, this is often referred to as a "$\pi-\pi$ stacking interaction", and these interactions have also been widely recognized as important in biological systems.[22−25] Herein, a very simple and cheap experiment is described that visualizes intermolecular $\pi-\pi$ stacking interactions.

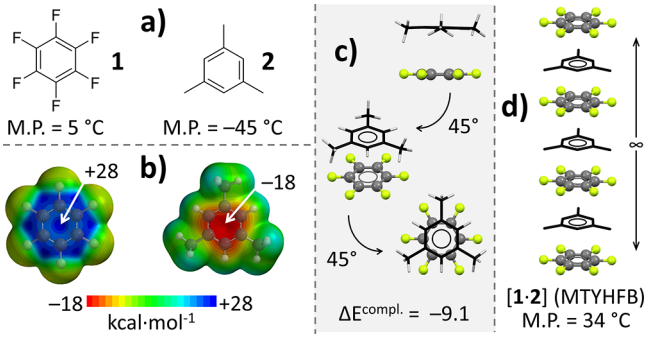

Figure 1. Aromatic molecules hexafluorobenzene (**1**) and 1,3,5-trimethylbenzene (**2**, mesitylene) and their melting points (a). In panel b, the molecular electrostatic potential maps of **1** and **2** visualize their polarization. Shown in panel c are three rotated perspective views of one [**1**·**2**] adduct that was geometry optimized using density functional theory (gas phase) with complexation energy (ΔE^{compl}) in kcal mol^{-1}. Shown in panel d is part of the infinite alternating stacking pattern observed in a crystal structure of [**1**·**2**]. The C atoms in the adduct (c, d) are gray for **1** and black for **2**. Hydrogen is white, and fluorine is green. See Materials and Methods for computational details.

Received: October 9, 2020
Revised: November 10, 2020
Published: December 4, 2020

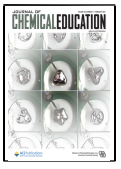

THE DEMONSTRATION

Background of the Experiment

To show an example of $\pi-\pi$ stacking interactions in a supramolecular chemistry course, we highlight the aromatic molecules hexafluorobenzene and mesitylene (**1** and **2** in Figure 1a). The molecular electrostatic potential maps of **1** and **2** are shown in Figure 1b and make it intuitively clear that **1** is π-acidic (blue center, indicating electron depletion), while **2** is π-basic (red center, indicating electron density). The $\pi-\pi$ stacked dimer can be geometry optimized (Figure 1c) with density functional theory (DFT), which indicates a complexation energy (ΔE^{compl}) of −9.1 kcal mol^{-1} in the gas phase. This is about 1.5 times larger than the interaction energy of a H-bonded water dimer calculated with the same method (−6.3 kcal mol^{-1}, details not given)[26−28] and thus on the order of a strong hydrogen bond.[29,30] Given these data, it is not surprising that **1** and **2** can form a cocrystal comprising infinite one-dimensional $\pi-\pi$ stacks between **1** and **2**, as is illustrated in Figure 1d (CSD refcode MTYHFB03).[31,32] The melting point of the cocrystal (34 °C)[32] is much higher than the melting points of **1** (5 °C)[33] and **2** (−45 °C),[34] thus illustrating the stabilizing effect of the $\pi-\pi$ stacking interactions.

The Experiment

At room temperature (typically 20−25 °C), **1** and **2** are clear, colorless liquids while their cocrystal should be a solid. This implies that mixing **1** and **2** could be a very easy visual experiment to demonstrate the relevance of intermolecular $\pi-\pi$ stacking interactions. Indeed, mixing equimolar amounts of **1** (10 mL) and **2** (12 mL) immediately resulted in the formation of a white crystalline solid under the evolution of heat. Photos of **1** and **2** before and after mixing are shown in Figure 2, and video of this process is given as Supporting Information. The demonstration has been performed in a lecture theater for first year MSc chemistry students to aid their appreciation of noncovalent interactions.

Figure 2. Photos of 10 mL of hexafluorobenzene (**1**) and 12 mL of mesitylene (**2**), together with the mixture (right). See Supporting Information for a video of the process (also on different scales).

Availability, Safety, Robustness, and Scale

Some details of **1** and **2** and several experimental conditions that were tried are collected in Table 1. What makes this demonstration particularly attractive is not only that it is visual, but also that it is trivial to perform, and that **1** and **2** are cheap, widely available, and relatively nontoxic. Indeed, 10 mL of **1** is about $9, and 10 mL of **2** costs less than a dollar, which adds up to about $10 for the experiment shown in Figure 2. Most chemical laboratories likely have some of both compounds, as **1** is often used as a cheap aromatic solvent for NMR and **2** is frequently used as an internal standard in both gas chromatography and NMR spectroscopy. Although both **1** and **2** are highly flammable irritants, their toxicity is on par with that of toluene (see footnote a of Table 1). On the basis of the oral LD_{50} values for rat, even a child of about 30 kg would have to ingest more than 150 g of either substance to have a 50% chance of dying, a scenario probably cut short by the unpleasant sensation these irritants likely induce. Nevertheless, both aromatics should obviously be kept away from children and handled with proper care (gloves and goggles are recommended).

Table 1. Some Information about Hexafluorobenzene (1) and Mesitylene (2) and the Volume and Molar Ratios Tested with Indicated Outcomes

	C_6F_6 (**1**)	$C_6H_3(CH_3)_3$ (**2**)
CAS	392-56-3	108-67-8
MW (g/mol)	186.056	120.190
ρ (g/cm^3)	1.6120	0.8637
bp (°C)	80	165
mp (°C)	5	−45
LD_{50} (or.)[a]	>10 g/kg[d]	6 g/kg
LD_{50} (der)[a]	n.a.	>2 g/kg
LC_{50} (inh)[a]	0.95 mg/L (2 h)	10.2 mg/L (4 h)
price/10 mL[b]	9−14	0.7−0.9

Volume Ratio in mL of **1**:**2**	Molar Equivalents of **1**:**2**	Outcome of Mixing[c]
0.9:0.1	10.85[e]	→ no
0.8:0.2	4.82[e]	→ no
0.7:0.3	2.81[e,f]	→ ±
0.6:0.4	1.81[e,f]	→ yes
0.5:0.5	1.21[e,g]	→ yes
0.5:0.6	1.00[e]	→ yes
0.4:0.6	0.80[e]	→ yes
0.3:0.7	0.52[e,f]	→ yes
0.2:0.8	0.30[e]	→ ±
0.1:0.9	0.13[e]	→ no
1.0:1.2	1.00[e]	→ yes
5.0:6.0	1.00[h]	→ yes
10:12	1.00[h]	→ yes[i]
25:30	1.00[h]	→ yes[i]

[a]Found online via https://chemicalsafety.com/sds-search/. or. = oral. der = dermal. inh = inhalation. All numbers are for rat, except the LC_{50} value for **1** (mice). For comparison purposes, the values for toluene are as follows: LD_{50} (oral), 5.58 g/kg (rat); LD_{50} (dermal), 12.2 g/kg (rabbit); LC_{50} (inhalation), 12.5 mg/L (4 h, rat). [b]Price ranges are from British pounds to US dollars (the Euro price will be in between). The price for **1** is calculated on the basis of a 500 g batch from Fluorochem (£144, 97% pure); the price of **2** is calculated on the basis of a 2.5 L batch from Sigma-Aldrich (€185, 98% pure). [c]The visual outcome of mixing was either the formation of a white crystalline solid (no), a clear colorless solution (yes), or the formation of crystals in a liquid (±) (cf., Figure S2). [d]Found via https://scifinder.cas.org/. [e]Mesitylene was added to hexafluorobenzene using a syringe. [f]The small amount of heat produced appeared to be sufficient to delay crystallization. [g]The experiment also worked when the volume of hexafluorobenzene was added to the vial with mesitylene and *vice versa*. [h]The volumes of both liquids were measured using a measuring cylinder and then mixed together in a vial/beaker/test tube. [i]A solid is formed directly after mixing, but there was a significant amount of heat produced which apparently dissipated slowly so that the mixture only fully solidified after more than an hour.

https://dx.doi.org/10.1021/acs.jchemed.0c01252
J. Chem. Educ. 2021, 98, 540−545

Another attractive feature of the demonstration is that it is rather robust; molar ratios of **1** versus **2** in the range 1:2−2:1 reliably give a visual effect when tested at a scale of ∼1 mL total volume (see Table 1). Experiments using a molar ratio of unity were also done on 2.2, 11, 22, and 55 mL total volumes (see also Figure S1), which all resulted in the nearly immediate formation of the crystalline solid. Movies of the experiments with ≥2 mL are provided as Supporting Information. In all experiments, the heat evolved was clearly sensible by hand. The temperature of an experiment at 55 mL total volume increased from 24.1 to 35.7 °C in about 1 min after adding **2** to a stirred batch of **1** (see Supporting Information). The temperature of this slurry remained at ∼36 °C for about 8 min and very slowly cooled back to room temperature, resulting in a white solid. The fact that this experiment is easily scaled up or down makes it feasible to perform the demonstration for a larger audience or have individual students perform the experiment. It must be noted that there is a substantial difference in the densities of **1** (ρ = 1.6120 g/cm^3) and **2** (ρ = 0.8637 g/cm^3) which can hinder efficient mixing in narrow tubes and thus delay the formation of the solid. This is evident from the two movies at 11 mL total volume using a 20 mL test tube (see Supporting Information): subsequent addition of **1** to **2** gave two layers that had to be mixed before crystallization ensued, while simultaneous addition immediately gave a solid.

Variations Such as Aromatics Other Than 2

For more advanced students, the demonstration could easily be expanded by linking it to other physical experiments such as measurement of the heat of formation of the cocrystal, measurement of the phase transition of melting the crystals, or a (azeotropic?) distillation, just to name a few. Another variation can be to link such experiments to a computational evaluation, which can nowadays be done on most desktop computers. Care must be taken to select the appropriate computational method that can give a reliable estimate of the binding enthalpy at a reasonable computational cost. To aid such considerations, Table S1 lists the interactions energies of [**1**···**2**] computed using molecular mechanics and semi-empirical and various density functional methods. These data make clear that dispersion corrected DFT methods must be used with an appropriate basis set (TPSS-D3/cc-pVTZ is fastest). Students could also investigate if other aromatics can be used to create a similar effect (possibly in conjunction with calculations). The liquid candidates that we tested bear resemblance to **2** and are shown in Figure 3, ordered by their melting points. Also indicated in the figure is whether mixing with an equimolar amount of **1** and the indicated aromatic resulted in the formation of a solid, the melting point of this solid, their price in USD per 10 mL, and the complexation energy (ΔE^{compl}) of the $\pi-\pi$ stacked dimer with **1** computed by DFT (see also Figure S3).

Mixing **1** and *p*-xylene (mp = 13 °C)[35] produced an odd wet crystalline compound upon slight agitation with a melting point around laboratory temperature (∼25 °C, see also Figure S4); warming by hand gave a clear solution, while in the fridge (5 °C) a white solid formed during cooling. The crystal structure of the $\pi-\pi$ stacked [**1**·*p*-xylene] columns is known (CSD refcode PXYHFB).[36,37] Using benzene (mp = 5.5 °C)[38] did not result in the formation of a solid (see Figure S4), although slight cooling did initiate crystallization (the sample turned solid when refrigerated at 5 °C). The solid formed is probably the $\pi-\pi$ stacked [**1**·benzene] structure that has been

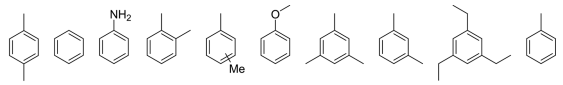

M.P.	13	5.5	−6.0	−25	−34	−37	−45	−48	−66.5	−93
Solid?	±	±	✓	✓	×	×	✓	×	×	×
M.P. of solid	26	25	43	38	u.k.	u.k.	34	u.k.	u.k.	u.k.
$ / 10ml	0.6	1.0	0.8	1.2	0.4	0.8	0.8	1.4	79	0.4
$\Delta E^{compl.}$	−8.2	−6.1	−8.0	−7.9	n.r.	−8.3	−9.1	−8.0	−9.5	−7.3

Figure 3. Mixtures of 0.5 mL of **1** with an equimolar amount of the π-basic components at room temperature with results indicating whether a solid formed (√) or not (X), or whether a solid formed with a melting point very close to the laboratory temperature of 25 °C (±). See also Figure S4 for the vials with the end result. Melting points for the pure π-basic components are displayed below the respective structure. Also shown are the outcomes of mixing (i.e., if a solid formed), the melting points of the solid formed, and the prices of each liquid in USD based on the price of a 2.5 L batch from Acros Organics (except benzene and 1,3,5-triethylbenzene, which were taken from TCI America, sold in 500 and 25 mL batches, respectively). The complexation energies (ΔE^{compl}) computed with DFT are also provided (see Materials and Methods for details). An energy decomposition analysis of all the adducts is shown in Figure S3 and indicates that generally these adducts are mainly driven by dispersion (47−55%), followed by electrostatic interactions (33−40%) and orbital interactions (11−14%). Dimethylbenzene was a mixture of the different xylenes and ethylbenzene as evident from an NMR spectrum (see Figure S5). Melting points in °C and ΔE^{compl} in kcal mol^{-1}. uk = unknown; nr = not relevant.

reported previously (CSD refcodes BICVUE03 and YOWWUF), which has a melting point of 25 °C.[39] The melting points of the solids that can be obtained using *p*-xylene or benzene are thus less practical for the demonstration at a typical indoor temperature of ∼25 °C. Moreover, use of benzene must be discouraged as it is a known carcinogen.[40]

Both aniline (mp = −6 °C)[41] and *o*-xylene (mp = −25 °C)[42] showed rapid crystal formation upon mixing with **1** (see Figure S4), which is in line with the relatively high melting points of the cocrystals formed (43 and 38 °C, respectively, cf., Figure S6). Both are thus also suitable for the demonstration experiment, although aniline is acutely toxic (LD_{50} = 0.25 g/kg (rat, oral)) and *o*-xylene is less safe than **2** (LD_{50} = 3.6 g/kg (rat, oral) versus 6 g/kg for **2**) and generally less available in a standard laboratory setting. A movie of mixing **1** and *o*-xylene at a 55 mL total scale is provided as Supporting Information. The solidification process with *o*-xylene is faster than that with mesitylene, presumably due to the higher melting point of the adduct (38 °C versus 34 °C for [**1**·**2**]). Mixing **1** and *o*-xylene also produced a significant amount of heat, and the mixture warmed from 23.3 to 38.4 °C in about 3 min (stirring with a spatula was needed). The crystal structures **1** with either aniline or *o*-xylene are not present in the CSD.

None of the other aromatics tested gave a solid at room temperature when mixing with **1** (Figure S4). Upon cooling to 5 °C, however, the mixture of toluene and **1** also produced crystals, which are likely the known $\pi-\pi$ stacks present in the crystal structure of [**1**·toluene] (CSD refcode LOHBUI).[37] This indicates that $\pi-\pi$ stacking likely also occurs in all other samples, but that the melting points of the assemblies are lower than 5 °C. The reason why 1,3,5-triethylbenzene does not form a solid might be rationalized on the basis of the fact that the ethyl groups in the energy minimum conformer point toward one side of the benzene core (see Figure S7). This likely facilitates the formation of a $\pi-\pi$ stacking geometry (ΔE^{compl} is the largest calculated at −9.5 kcal mol^{-1}) but prevents the formation of infinite 1-dimensional stacks such as

https://dx.doi.org/10.1021/acs.jchemed.0c01252
J. Chem. Educ. 2021, 98, 540−545

those observed in [**1**·benzene] and [**1**·mesitylene]. Crystal structures of **1** with anisole, *m*-xylene, and 1,3,5-triethylbenzene are not present in the CSD.

Interestingly, the system is sensitive to competitive $\pi-\pi$ stacking as the mixture of xylenes that consists mostly of *m*-xylene (49%) and *p*-xylene (24%) did not produce crystals, not even when cooled to 5 °C (see Figure S5 for an NMR spectrum of the xylene mixture).

A final observation from the data collected in Figure 3 is that neither the melting point of the aromatic nor the computed complexation energies seem to be a clear predictor of whether an equimolar mixture with **1** will produce a crystalline solid. This could be used to initiate an interesting conversation with graduate students. Some additional computational data such as an energy decomposition analysis are provided in Figure S3 and indicate that all adducts are mainly driven by dispersion (47−55%), followed by electrostatic interactions (33−40%) and orbital interactions (11−14%).

Literature Discussion and Conclusion

To teach students about noncovalent (intermolecular) interactions, there is ample material available in the form of books and (review) articles.[1−25] There are several articles aimed specifically at teaching intermolecular interactions using conceptual (and computational) teaching methods.[43−53] There are also many articles describing experiments based on physical properties such as vapor pressure, polarity, boiling point, phase behavior, and salting properties.[54−66] One article was found describing the solvent dependent luminescence of 3-hydroxyflavone (at −196 °C) based on intra- versus intermolecular hydrogen bonding,[67] and one paper describes an experiment based on protein−protein binding.[68] While very insightful, the experiments cited are relatively difficult and expensive to set up, and their execution can be too lengthy for the purposes of a simple demonstration.

In conclusion, the formation of the [**1**·**2**] cocrystal is a rarely quick, easy, inexpensive, safe, and robust experiment to demonstrate the existence and the effect of $\pi-\pi$ stacking interactions.

MATERIALS AND METHODS

Aromatics **1** (97% pure) and **2** (98% pure) were purchased from Fluorochem and Sigma-Aldrich, respectively, and used as received. Benzene (>99.5% pure from TCI), aniline (99% pure from Sigma-Aldrich), toluene (>99.5% pure from VWR), *o*-xylene (99% pure from Acros Organics), *p*-xylene (>99% pure from TCI), *m*-xylene (99+% pure from Aldrich), xylenes (99% pure from Acros Organics), 1,3,5-triethylbenzene (98% pure from Aldrich), and anisole (99% pure from Sigma-Aldrich) were also used as received. DFT geometry optimization calculations were performed with Spartan 2016 at the B3LYP[69,70]-D3[71]/def2-TZVP[72,73] level of theory, which is known to give accurate results at reasonable computational cost and a very low basis set superposition error (BSSE).[71−73] The molecular fragments were manually oriented in a suitable constellation before starting an unconstrained geometry optimization. Individual molecules were also optimized separately, and the energy difference between those and the energy of the adduct is the complexation energy (ΔE^{compl}). Spartan was also used to calculate the molecular electrostatic potential maps. The Amsterdam density functional (ADF)[74] modeling suite at the B3LYP[69,70]-D3[71]/TZ2P[72,73] level of theory (no frozen cores) was used to compute the reported BSSE corrected interaction energies (ΔE^{BSEE}, using the "ghost atoms" option for counterpoise correction) of the optimized structures reported in Figure S3. The ΔE^{BSEE} energy does not include the deformation energy. ADF was likewise used to compute the energy decomposition and "atoms in molecules"[75] analyses (using the default ADF settings). Details of the Morokuma−Ziegler inspired energy decomposition scheme (also given in Figure S3) used in the ADF-suite have been reported elsewhere,[74,76] and the scheme has proven useful to evaluate hydrogen bonding interactions.[77,78]

ASSOCIATED CONTENT

Supporting Information

The Supporting Information is available at https://pubs.acs.org/doi/10.1021/acs.jchemed.0c01252.

Results of mixing **1** and **2** at various scales; results of mixing **1** and **2** at various ratios; DFT calculations of adducts between **1** and various π-basic aromatics; results of mixing **1** with various aromatics; ^{1}H NMR spectra of the dimethylbenzene mixture used; melting curves for crystals of **1** with mesitylene, *o*-xylene, and aniline; and DFT calculations of three conformers of 1,3,5-triethylbenzene; and interaction energies of [**1**···**2**] computed with various methods (PDF, DOCX)

Video showing addition of **2** to **1** at 2.2 mL total volume (MP4)

Video showing addition of **2** to **1** at 11 mL total volume (MP4)

Video showing simultaneous mixing of **2** and **1** at 11 mL total volume (MP4)

Video showing addition of **2** to **1** at 22 mL total volume (MP4)

Video showing addition of **2** to **1** at 55 mL total volume (MP4)

Video showing addition of *o*-xylene to **1** at 55 mL total volume (MP4)

AUTHOR INFORMATION

Corresponding Author

Tiddo Jonathan Mooibroek − *van't Hoff Institute for Molecular Sciences, Universiteit van Amsterdam, 1098 XH Amsterdam, The Netherlands;* orcid.org/0000-0002-9086-1343; Email: t.j.mooibroek@uva.nl

Author

Brian Jacobus Jozefus Timmer − *van't Hoff Institute for Molecular Sciences, Universiteit van Amsterdam, 1098 XH Amsterdam, The Netherlands;* orcid.org/0000-0002-9458-4822

Complete contact information is available at: https://pubs.acs.org/10.1021/acs.jchemed.0c01252

Notes

The authors declare no competing financial interest.

ACKNOWLEDGMENTS

T.J.M. thanks NWO (VIDI project 723.015.006) for funding.

REFERENCES

(1) Schneider, H. J. *Supramolecular Systems in Biomedical Fields*, 1st ed.; RSC Publishing: Cambridge, UK, 2013.

(2) Cragg, P. J. *Supramolecular Chemistry: From Biological Inspiration to Biomedical Applications*, 1st ed.; Springer: Dordrecht, 2010.
(3) Bruce, A.; Johnson, A. D.; Lewis, J.; Morgan, D.; Raff, M.; Roberts, K.; Walter, P. *Molecular Biology of the Cell*, 6th ed.; Garland Science (Taylor & Francis Group): New York, 2015.
(4) Wang, Q. H.; Zhang, Y. F.; Wu, L. L.; Niu, S.; Song, C. L.; Zhang, Z. Y.; Lu, G. W.; Qiao, C. P.; Hu, Y.; Yuen, K. Y.; Wang, Q. S.; Zhou, H.; Yan, J. H.; Qi, J. X. Structural and functional basis of SARS-CoV-2 entry by using human ACE2. *Cell* **2020**, *181* (4), 894−904.
(5) Metrangolo, P.; Neukirch, H.; Pilati, T.; Resnati, G. Halogen bonding based recognition processes: a world parallel to hydrogen bonding. *Acc. Chem. Res.* **2005**, *38* (5), 386−395.
(6) Bissantz, C.; Kuhn, B.; Stahl, M. A medicinal chemist's guide to molecular interactions. *J. Med. Chem.* **2010**, *53* (14), 5061−5084.
(7) Bauza, A.; Mooibroek, T. J.; Frontera, A. The bright future of unconventional σ/π-hole interactions. *ChemPhysChem* **2015**, *16* (12), 2496−2517.
(8) Politzer, P.; Murray, J. S.; Clark, T.; Resnati, G. The σ-hole revisited. *Phys. Chem. Chem. Phys.* **2017**, *19* (48), 32166−32178.
(9) Lehn, J. M. *Supramolecular Chemistry: Concepts and Perspectives*, 1st ed.; Wiley VCH: Weinheim, 1995.
(10) Steed, J. W.; Atwood, J. L. *Supramolecular Chemistry*; Wiley: Chichester, 2000.
(11) Bartlett, G. J.; Choudhary, A.; Raines, R. T.; Woolfson, D. N. $n\rightarrow\pi^*$ interactions in proteins. *Nat. Chem. Biol.* **2010**, *6* (8), 615−620.
(12) Bauza, A.; Alkorta, I.; Elguero, J.; Mooibroek, T. J.; Frontera, A. Spodium bonds: noncovalent interactions involving group 12 elements. *Angew. Chem., Int. Ed.* **2020**, *59*, 17482.
(13) Heywood, V. L.; Alford, T. P. J.; Roeleveld, J. J.; Lekanne Deprez, S. J.; Verhoofstad, A.; van der Vlugt, J. I.; Domingos, S. R.; Schnell, M.; Davis, A. P.; Mooibroek, T. J. Observations of tetrel bonding between sp^3-carbon and THF. *Chem. Sci.* **2020**, *11* (20), 5289−5293.
(14) Hunter, C. A.; Lawson, K. R.; Perkins, J.; Urch, C. J. Aromatic interactions. *J. Chem. Soc.-Perkin Trans. 2* **2001**, No. 5, 651−669.
(15) Asensio, J. L.; Arda, A.; Canada, F. J.; Jimenez-Barbero, J. Carbohydrate-aromatic interactions. *Acc. Chem. Res.* **2013**, *46* (4), 946−954.
(16) Carter, T. S.; Mooibroek, T. J.; Stewart, P. F. N.; Crump, M. P.; Galan, M. C.; Davis, A. P. Platform synthetic lectins for divalent carbohydrate recognition in water. *Angew. Chem., Int. Ed.* **2016**, *55* (32), 9311−9315.
(17) Frontera, A.; Gamez, P.; Mascal, M.; Mooibroek, T. J.; Reedijk, J. Putting anion-π interactions into perspective. *Angew. Chem., Int. Ed.* **2011**, *50* (41), 9564−9583.
(18) Schottel, B. L.; Chifotides, H. T.; Dunbar, K. R. Anion-π interactions. *Chem. Soc. Rev.* **2008**, *37* (1), 68−83.
(19) Mooibroek, T. J.; Gamez, P.; Reedijk, J. Lone pair-π interactions: a new supramolecular bond? *CrystEngComm* **2008**, *10* (11), 1501−1515.
(20) Meyer, E. A.; Castellano, R. K.; Diederich, F. Interactions with aromatic rings in chemical and biological recognition. *Angew. Chem., Int. Ed.* **2003**, *42* (11), 1210−1250.
(21) Salonen, L. M.; Ellermann, M.; Diederich, F. Aromatic rings in chemical and biological recognition: energetics and structures. *Angew. Chem., Int. Ed.* **2011**, *50* (21), 4808−4842.
(22) Hunter, C. A.; Singh, J.; Thornton, J. M. π-π interactions - the geometry and energetics of phenylalanine phenulalanine interactions in proteins. *J. Mol. Biol.* **1991**, *218* (4), 837−846.
(23) Mignon, P.; Loverix, S.; Steyaert, J.; Geerlings, P. Influence of the π-π interaction on the hydrogen bonding capacity of stacked DNA/RNA bases. *Nucleic Acids Res.* **2005**, *33* (6), 1779−1789.
(24) Vernon, R. M.; Chong, P. A.; Tsang, B.; Kim, T. H.; Bah, A.; Farber, P.; Lin, H.; Forman-Kay, J. D. π-π contacts are an overlooked protein feature relevant to phase separation. *eLife* **2018**, *7*, No. e31486.
(25) McGaughey, G. B.; Gagne, M.; Rappe, A. K. π-stacking interactions - alive and well in proteins. *J. Biol. Chem.* **1998**, *273* (25), 15458−15463.
(26) Klopper, W.; van Duijneveldt-van de Rijdt, J.; van Duijneveldt, F. B. Computational determination of equilibrium geometry and dissociation energy of the water dimer. *Phys. Chem. Chem. Phys.* **2000**, *2* (10), 2227−2234.
(27) Reinhardt, P.; Piquemal, J. P. New Intermolecular Benchmark Calculations on the Water Dimer: SAPT and Supermolecular Post-Hartree-Fock Approaches. *Int. J. Quantum Chem.* **2009**, *109* (14), 3259−3267.
(28) Andric, J. M.; Janjic, G. V.; Ninkovic, D. B.; Zaric, S. D. The influence of water molecule coordination to a metal ion on water hydrogen bonds. *Phys. Chem. Chem. Phys.* **2012**, *14* (31), 10896−10898.
(29) Biedermann, F.; Schneider, H.-J. Experimental binding energies in supramolecular complexes. *Chem. Rev.* **2016**, *116* (9), 5216−5300.
(30) Nemethy, G.; Pottle, M. S.; Scheraga, H. A. Energy parameters in polypeptides. 9. Updating of geometrical parameters, nonbonded interactions, and hydrogen-bond interactions for the naturally-occurring amino-acids. *J. Phys. Chem.* **1983**, *87* (11), 1883−1887.
(31) Dahl, T.; Gropen, O.; Wilhelmi, K.-A.; Lindberg, A. A.; Lagerlund, I.; Ehrenberg, L. Crystal structure of the 1:1 complex between mesitylene and hexafluorobenzene. *Acta Chem. Scand.* **1971**, *25*, 1031−1039.
(32) Cockcroft, J. K.; Ghosh, R. E.; Shephard, J. J.; Singh, A.; Williams, J. H. Investigation of the phase behaviour of the 1:1 adduct of mesitylene and hexafluorobenzene. *CrystEngComm* **2017**, *19* (7), 1019−1023.
(33) Ott, J. B.; Goates, F. R.; Cardon, D. L. Enthalpies of formation of the *p*-xylene + carbon tetrachloride and the benzene + hexafluorobenzene solid addition compounds. *J. Chem. Thermodyn.* **1976**, *8*, 505−512.
(34) Shinsaka, K.; Freeman, G. R. Epithermal electron ranges and thermal electron mobilities in liquid aromatic hydrocarbons. *Can. J. Chem.* **1974**, *52* (20), 3495−3506.
(35) Messerly, J. F.; Finke, H. L.; Good, W. D.; Gammon, B. E. Condensed-phase heat capacities and derived thermodynamic properties for 1,4-dimethylbenzene, 1,2-diphenylethane, and 2,3-dimethylnaphthalene. *J. Chem. Thermodyn.* **1988**, *20* (4), 485−501.
(36) Dahl, T.; Marøy, K.; Slogvik, S.; Southern, J. T.; Southern, J. T.; Edlund, K.; Eliasen, M.; Herskind, C.; Laursen, T.; Pedersen, P. Møl. Crystal-structure of 1−1 addition compound between *p*-xylene and hexafluorobenzene. *Acta Chem. Scand.* **1975**, *29a* (2), 170−174.
(37) Cockcroft, J. K.; Li, J. G. Y.; Williams, J. H. Influence of methyl-substitution on the dynamics of the C-H center dot center dot center dot F-C interaction in binary adducts. *CrystEngComm* **2019**, *21* (37), 5578−5585.
(38) Goates, J. R.; Ott, J. B.; Moellmer, J. F.; Farrell, D. W. (solid + liquid) Phase-equilibria in *n*-hexane - cyclohexane and benzene + *p*-xylene. *J. Chem. Thermodyn.* **1979**, *11* (7), 709−711.
(39) Cockcroft, J. K.; Rosu-Finsen, A.; Fitch, A. N.; Williams, J. H. The temperature dependence of C-H···F-C interactions in benzene:-hexafluorobenzene. *CrystEngComm* **2018**, *20* (42), 6677−6682.
(40) Huff, J. Benzene-induced cancers: abridged history and occupational health impact. *Int. J. Occup. Environ. Health* **2007**, *13* (2), 213−221.
(41) Fukuyo, M.; Hirotsu, K.; Higuchi, T. The structure of aniline at 252 K. *Acta Crystallogr. Sect. B-Struct. Commun.* **1982**, *38*, 640−643.
(42) Martin, E.; Wells, J. E.; Yalkowsky, S. H. Fusion of disubstituted benzenes. *J. Pharm. Sci.* **1979**, *68* (5), 565−568.
(43) Frieden, E. Noncovallent interacions - key to biological flexibility and specificity. *J. Chem. Educ.* **1975**, *52* (12), 754−761.
(44) Campanario, J. M.; Bronchalo, E.; Hidalgo, M. A. An effective approach for teaching intermolecular interactions. *J. Chem. Educ.* **1994**, *71* (9), 761−766.
(45) Williams, L. C.; Underwood, S. M.; Klymkowsky, M. W.; Cooper, M. M. Are noncovalent interactions an achilles heel in

https://dx.doi.org/10.1021/acs.jchemed.0c01252
J. Chem. Educ. 2021, 98, 540−545

chemistry education? A comparison of instructional approaches. *J. Chem. Educ.* **2015**, *92* (12), 1979−1987.
(46) Murthy, P. S. Molecular handshake: recognition through weak noncovalent interactions. *J. Chem. Educ.* **2006**, *83* (7), 1010−1013.
(47) Cox, J. R. Teaching noncovalent interactions in the biochemistry curriculum through molecular visualization: the search for π interactions. *J. Chem. Educ.* **2000**, *77* (11), 1424−1428.
(48) Bruist, M. F. A simple demonstration of how intermolecular forces make DNA helical. *J. Chem. Educ.* **1998**, *75* (1), 53−55.
(49) Battle, G. M.; Allen, F. H. Learning about intermolecular interactions from the Cambridge structural database. *J. Chem. Educ.* **2012**, *89* (1), 38−44.
(50) Peckham, G. D.; McNaught, I. J. Teaching intermolecular forces to first-year undergraduate students. *J. Chem. Educ.* **2012**, *89* (7), 955−957.
(51) Weinhold, F.; Klein, R. A. What is a hydrogen bond? Resonance covalency in the supramolecular domain. *Chem. Educ. Res. Pract.* **2014**, *15* (3), 276−285.
(52) Cooper, A. K.; Oliver-Hoyo, M. T. Argument construction in understanding noncovalent interactions: a comparison of two argumentation frameworks. *Chem. Educ. Res. Pract.* **2016**, *17* (4), 1006−1018.
(53) Loertscher, J.; Lewis, J. E.; Mercer, A. M.; Minderhout, V. Development and use of a construct map framework to support teaching and assessment of noncovalent interactions in a biochemical context. *Chem. Educ. Res. Pract.* **2018**, *19* (4), 1151−1165.
(54) Fitzgerald, J. P.; Ferrante, R. F.; Brown, M.; Cabarrus, J. Relating ΔH_{vap} of organic liquids to intermolecular forces: simple modifications of a classic general chemistry experiment. *J. Chem. Educ.* **2020**, *97* (5), 1406−1410.
(55) Cunningham, W. P.; Xia, I.; Wickline, K.; Garcia Huitron, E. I.; Heo, J. Studying intermolecular forces with a dual gas chromatography and boiling point investigation. *J. Chem. Educ.* **2018**, *95* (2), 300−304.
(56) Ogden, M. An inquiry experience, with high school students to develop an understanding of intermolecular forces by relating boiling point trends and molecular structure. *J. Chem. Educ.* **2017**, *94* (7), 897−902.
(57) Struyf, J. An analytical approach for relating boiling points of monofunctional organic compounds to intermolecular forces. *J. Chem. Educ.* **2011**, *88* (7), 937−943.
(58) Csizmar, C. M.; Force, D. A.; Warner, D. L. Implementation of gas chromatography and microscale distillation into the general chemistry laboratory curriculum as vehicles for examining intermolecular forces. *J. Chem. Educ.* **2011**, *88* (7), 966−969.
(59) Wedvik, J. C.; McManaman, C.; Anderson, J. S.; Carroll, M. K. Intermolecular forces in introductory chemistry studied by gas chromatography, computer models, and viscometry. *J. Chem. Educ.* **1998**, *75* (7), 885−888.
(60) Beauvais, R.; Holman, R. W. An internal comparison of the intermolecular forces of common organic functional groups - a thin layer chromatography experiment. *J. Chem. Educ.* **1991**, *68* (5), 428−429.
(61) Berka, L. H.; Kildahl, N. Experiments for modern introductory chemistry - intermolecular forces and Raoult law. *J. Chem. Educ.* **1994**, *71* (7), 613−616.
(62) Jasien, P. G. Helping students assess the relative importance of different intermolecular interactions. *J. Chem. Educ.* **2008**, *85* (9), 1222−1225.
(63) Mundell, D. W. Dancing crystals: a dramatic illustration of intermolecular forces. *J. Chem. Educ.* **2007**, *84* (11), 1773−1775.
(64) Cannon, A. S.; Warner, J. C.; Koraym, S. A.; Marteel-Parrish, A. E. Noncovalent derivatization: a laboratory experiment for understanding the principles of molecular recognition and self-assembly through phase behavior. *J. Chem. Educ.* **2014**, *91* (9), 1486−1490.
(65) Person, E. C.; Golden, D. R.; Royce, B. R. Salting effects as an illustration of the relative strength of intermolecular forces. *J. Chem. Educ.* **2010**, *87* (12), 1332−1335.
(66) Schmidt, H. J.; Kaufmann, B.; Treagust, D. F. Students' understanding of boiling points and intermolecular forces. *Chem. Educ. Res. Pract.* **2009**, *10* (4), 265−272.
(67) Ni, C. W.; Lin, G. Y.; Wang, T. Y.; Ho, M. L. Using luminescence to show intramolecular and intermolecular hydrogen bonding: an activity for general chemistry or physical chemistry. *J. Chem. Educ.* **2015**, *92* (2), 322−327.
(68) Johnson, S. M.; Javner, C.; Hackel, B. J. Development and implementation of a protein-protein binding experiment to teach intermolecular interactions in high school or undergraduate classrooms. *J. Chem. Educ.* **2017**, *94* (3), 367−374.
(69) Becke, A. D. Density-functional exchange-energy approximation with correct asymptotic-behaviour. *Phys. Rev. A: At., Mol., Opt. Phys.* **1988**, *38* (6), 3098−3100.
(70) Lee, C. T.; Yang, W. T.; Parr, R. G. Development of the Colle-Salvetti correlation-energy formula into a functional of the electron density. *Phys. Rev. B: Condens. Matter Mater. Phys.* **1988**, *37* (2), 785−789.
(71) Grimme, S.; Antony, J.; Ehrlich, S.; Krieg, H. A consistent and accurate ab initio parametrization of density functional dispersion correction (DFT-D) for the 94 elements H-Pu. *J. Chem. Phys.* **2010**, *132* (15), No. 154104.
(72) Weigend, F.; Ahlrichs, R. Balanced basis sets of split valence, triple zeta valence and quadruple zeta valence quality for H to Rn: design and assessment of accuracy. *Phys. Chem. Chem. Phys.* **2005**, *7* (18), 3297−3305.
(73) Weigend, F. Accurate Coulomb-fitting basis sets for H to Rn. *Phys. Chem. Chem. Phys.* **2006**, *8* (9), 1057−1065.
(74) te Velde, G.; Bickelhaupt, F. M.; Baerends, E. J.; Fonseca Guerra, C.; van Gisbergen, S. J. A.; Snijders, J. G.; Ziegler, T. Chemistry with ADF. *J. Comput. Chem.* **2001**, *22* (9), 931−967.
(75) Bader, R. F. W. Atoms in molecules. *Acc. Chem. Res.* **1985**, *18* (1), 9−15.
(76) Bickelhaupt, F. M.; Baerends, E. J. Kohn-Sham Density Functional Theory: Predicting and Understanding Chemistry. In *Reviews in Computational Chemistry*; Lipkowitz, K. B., Boyd, D. B., Eds.; Wiley-VCH, Inc.: New York, 2000; Vol. *15*, pp 1−86.
(77) van der Lubbe, S. C. C.; Fonseca Guerra, C. The nature of hydrogen bonds: a delineation of the role of different energy components on hydrogen bond strengths and lengths. *Chem. - Asian J.* **2019**, *14* (16), 2760−2769.
(78) Mooibroek, T. J. Intermolecular non-covalent carbon-bonding Interactions with Methyl Groups: a CSD, PDB and DFT Study. *Molecules* **2019**, *24* (18), No. 3370.

https://dx.doi.org/10.1021/acs.jchemed.0c01252
J. Chem. Educ. 2021, 98, 540−545